Journal of Solid State Chemistry **156,** 101–109 (2001)
doi:10.1006/jssc.2000.8968, available online at http://www.idealibrary.com on IDEAL®

Spin-1/2 Quantum Antiferromagnetic Chains with Tunable Superexchange Interactions Found in $BaCu_2(Si_{1-x}Ge_x)_2O_7$

T. Yamada,*[,1] Z. Hiroi,† and M. Takano*

** Institute for Chemical Research, Kyoto University, Uji, Kyoto 611-0011, Japan and † Institute for Solid State Physics, University of Tokyo, 5-1-5, Kashiwanoha, Kashiwa-shi, Chiba 277-8581, Japan*

Received May 8, 2000; in revised form August 29, 2000; accepted September 15, 2000; published online December 21, 2000

Synthesis, structure, and magnetic properties of a novel one-dimensional spin-1/2 quantum antiferromagnetic (AF) system $BaCu_2(Si_{1-x}Ge_x)_2O_7$ ($0 \le x \le 1$) are reported. Contained in this system are corrugated CuO chains made of corner-sharing CuO_4 squares with the dominant exchange interaction changing almost linearly between 290 K ($x = 0$) and 580 K ($x = 1$). Anomalies in susceptibility and specific heat, indicative of the occurrence of a long-range AF ordering, are observed at 8.9 K ($x = 0$) and 8.6 K ($x = 1$). A rich magnetic phase diagram results from this strong composition dependence combined with the switching of the interchain interaction changing from ferromagnetic ($x = 0$) to AF ($x = 1$).

Key Words: **$BaCu_2(Si_{1-x}Ge_x)_2O_7$; Heisenberg antiferromagnetic chains; corner-sharing CuO_4 squares; Dzyaloshinsky–Moriya interaction; Superexchange interactions.**

INTRODUCTION

One dimensional (1D) Heisenberg antiferromagnetic (HAF) spin systems are known to exhibit various exotic magnetism caused by large quantum fluctuations which suppress an ordinary long-range order (LRO). Recent extensive studies on 1D cupric oxides have revealed interesting phenomena such as the spin-Peierls transition in $CuGeO_3$ (1) and the spin-charge separation in $SrCuO_2$ (2).

Two kinds of Cu–O chains made of CuO_4 squares are known; a corner-sharing chain as seen in Sr_2CuO_3 and $SrCuO_2$ and an edge-sharing chain as in $CuGeO_3$, Li_2CuO_2, $(Ca,Sr)_{14}Cu_{24}O_{41}$, and $Ca_{1-x}CuO_2$. The former type exhibits a relatively large AF interaction, J, of the order of 10^3 K due to the strong Cu $3d$–O $2p$ mixing in the linear Cu–O–Cu bond, while the Cu–O–Cu bond bent to $\sim 90^\circ$ can be either AF or ferromagnetic (F). According to a theoretical study by Mizuno *et al.* (3), the nearest-neighbor (n.n.) interaction, J_1, depends sensitively on the bond angle θ in such a way that $J_1/k_B \sim -100$ K (F) for Li_2CuO_2 ($\theta \sim 94^\circ$) and 140 K (AF) for $CuGeO_3$ ($\theta = 99^\circ$). In contrast, the second n.n. interaction J_2 is always AF at 62 K for Li_2CuO_2 and 18 K for $CuGeO_3$, for example. In contrast, the bond-angle dependence of J for a corner-sharing chain has not yet been studied experimentally nor theoretically. This is mainly because it is difficult to find appropriate model compounds. Here we report on $BaCu_2Si_2O_7$, $BaCu_2Ge_2O_7$, and their solid solutions $BaCu_2(Si_{1-x}Ge_x)_2O_7$ which contain unique corner-sharing CuO chains bent to $\sim 130^\circ$.

The crystal structure of $BaCu_2Si_2O_7$ was solved by Janczak and Kuciak by means of the Rietveld analysis of the powder X-ray diffraction (XRD) profile (4), while the structure of $BaCu_2Ge_2O_7$ has not yet been reported. Very recently, Tsukada *et al.* prepared a single crystal of $BaCu_2Si_2O_7$ and reported its susceptibility and neutron scattering data (5). We have prepared polycrystalline samples of these two compounds as well as their solid solutions (6) and studied their structural and magnetic properties in detail. As a result, it is evidenced that they represent an outstanding 1D HAF system with a linearly tunable interaction between $J = 290$ K ($x = 0$) and 580 K ($x = 1$). This change must probably be correlated with the small change in the Cu–O–Cu bond angle from 121° ($x = 0$) to 128° ($x = 1$). In addition, it is suggested that an interchain coupling also depends on the Si/Ge composition, changing its sign from F ($x = 0$) to AF ($x = 1$). These remarkable composition dependences give rise to a rich magnetic phase diagram of the present system, as will be shown in a later section.

EXPERIMENTAL

A series of polycrystalline samples of $BaCu_2(Si_{1-x}Ge_x)_2O_7$ ($x = 0$, 0.025, 0.05, 0.075, 0.1, 0.15, 0.25, 0.5, 0.75, 0.9,

[1] To whom correspondence should be addressed. Fax: +81 791-58-0830. E-mail: takahiro@spring8.or.jp.

0022-4596/01 $35.00

0.95, 1) were prepared by a standard solid state reaction method as follows. An appropriate mixture of $BaCO_3$ (3 N), SiO_2 (3 N), GeO_2 (3 N), and CuO (4 N) powders was grounded in an agate mortar, pressed into a pellet, and calcined at 850°C in air for 12 h. The product was then treated several times at higher temperatures up to 1015°C for 50 h in total with intermittent grindings and pelletizations. After the final heat treatment the product was quenched to room temperature in air. Thus obtained samples showed blue color: bright blue for the Si-rich side and dark blue for the Ge-rich side. All the samples were electrically insulative.

The samples were examined by means of powder XRD with graphite-monochromated Cu$K\alpha$ radiation. The crystal structure was refined by means of the Rietveld analysis of the powder patterns using the software RIETAN (7). Data for this were collected at room temperature over a 2θ range 10–120° at a 0.02° step, each for 10 s. Magnetic susceptibility was measured on a Quantum Design SQUID magnetometer (MPMS-XL) typically in an applied field of 0.1 T from 2 to 400 K. Specific heat was measured between 2 and 30 K by a relaxation method in a quantum design physical property measurement system (PPMS).

RESULTS

3.1. $BaCu_2Si_2O_7$ and $BaCu_2Ge_2O_7$

Crystal structure. The previous study on $BaCu_2Si_2O_7$ gave an orthorhombic space group of *Pnma* with lattice dimensions of $a = 6.866$, $b = 13.190$, and $c = 6.906$ Å (4). Starting from the atomic coordinates given in the reference, we carried out the Rietveld analysis for both the Si and Ge phases. Figure 1 illustrates the results for $BaCu_2Ge_2O_7$ showing excellent fits between the observed and calculated patterns. The resulting structural parameters and their estimated standard deviations are listed in Tables 1 and 2. The lattice constants are $a = 6.86058(8)$, $b = 13.17507(17)$, and $c = 6.89589(8)$ Å for the Si compound, and $a = 7.04765(6)$, $b = 13.40700(9)$, and $c = 7.02755(5)$ Å for the Ge compound. The R factors are $R_{wp} = 1.65\%$, $R_e = 2.63\%$, $R_p = 1.24\%$, $R_B = 4.04\%$, and $R_F = 3.66\%$ for the Si compound, and $R_{wp} = 1.58\%$, $R_e = 2.80\%$, $R_p = 1.11\%$, $R_B = 2.27\%$, and $R_F = 1.40\%$ for the Ge compound. The goodness-of-fit index, R_{wp}/R_e, is 0.63 and 0.57, respectively. The obtained structural parameters for $BaCu_2Si_2O_7$ are in good agreement with the previous report. The small R factors for $BaCu_2Ge_2O_7$ confirmed that the Ge analogue is isostructural with the Si compound.

The crystal structure is illustrated schematically in Fig. 2. The key units are obviously CuO_4 squares (or flattened CuO_4 tetrahedra) and $(Si, Ge)_2O_7$ groups made of a pair of corner-shared $(Si, Ge)O_4$ tetrahedra. The CuO_4 squares are connected to each other by their corners, forming 1D chains along the c axis. Note that they are heavily corrugated to an intrachain Cu–O–Cu bond angle θ of 121.0° for Si and 128.4° for Ge. In the previous studies on a series of compounds with edge-sharing CuO_2 chains (3), it was pointed out that the superexchange coupling changes their sign depending upon the Cu–O–Cu bond angle from F ($\theta \leq 95°$) to AF ($\theta \geq 95°$). It is then expected that the chains with $\theta = 120$–130° in the present compounds possess rather large AF couplings, though these must be significantly smaller than those for the linear chains. A typical compound Sr_2CuO_3 comprising such corner-sharing chains presents the most idealistic 1D HAF system with a large J/k_B of 2200 K and a low Néel order temperature (T_N) of 5.4 K (8).

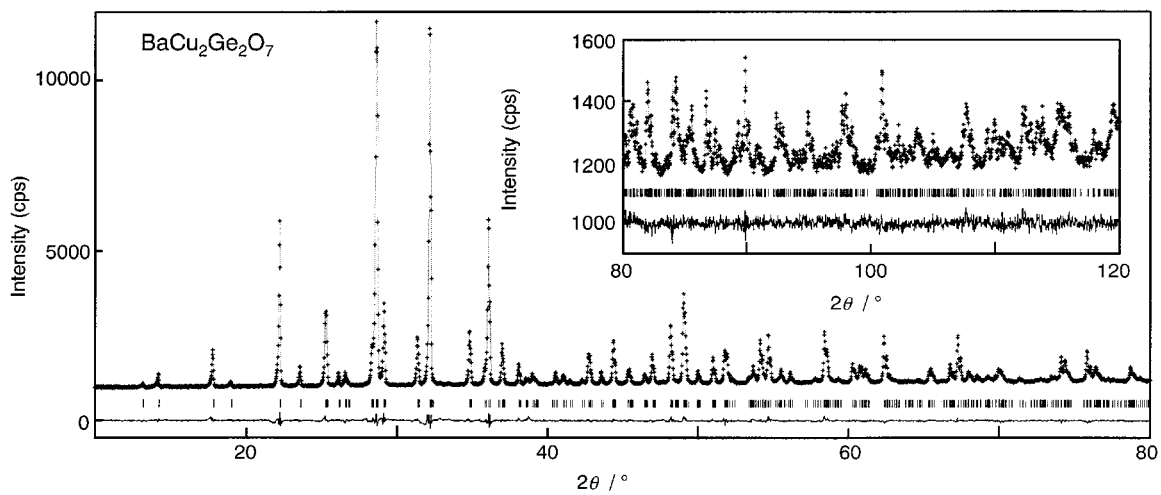

FIG. 1. Rietveld refinement patterns for $BaCu_2Ge_2O_7$. Observed diffraction intensities are represented by plus marks, and the calculated patterns by the solid lines. Differences between the observed and calculated intensities are given near the bottom. Short vertical marks indicate the position of allowed Bragg reflections.

TABLE 1
Fractional Atomic Coordinates and Atomic Displacement Parameters for $BaCu_2Si_2O_7$

Atom	Wyckoff position	x	y	z	B_{iso}(Å^2)
Ba	4c	− 0.0115(3)	0.25	0.9558(2)	1.77(4)
Cu	8d	0.2214(3)	0.0052(2)	0.7927(3)	1.80(6)
Si	8d	0.0045(9)	0.1337(2)	0.4732(6)	0.66(8)
O1	4c	0.0775(13)	0.25	0.4781(14)	− 0.01(30)
O2	8d	− 0.1617(13)	0.1311(8)	0.6238(12)	1.97(25)
O3	8d	− 0.0698(13)	0.1155(8)	0.2619(10)	2.33(30)
O4	8d	0.1809(9)	0.0649(5)	0.5299(12)	0.58(22)

Note. Space group *Pnma*; $a = 6.86058(8)$ Å, $b = 13.17507(17)$ Å, $c = 6.89589(8)$ Å; $Z = 4$.

Concerning the interchain couplings in the present compounds, it is likely that those along the b axis over a distance of 6.5 Å would be much weaker than those along the a axis.

Magnetic susceptibility. Figure 3 shows the temperature dependences of magnetic susceptibility χ for the two compounds measured in an applied field of 0.1 T. Each set of data exhibits a broad, rounded maximum, indicating the development of short-range AF correlations characteristic of low-dimensional HAF systems. However, the temperature of the maximum is quite different: 170 K for Si and 360 K for Ge. In addition, the magnitude of χ is greatly reduced for the latter. These facts imply that the intrachain interaction J is much larger for the Ge compound. The behavior at low temperature below the maximum is also quite different: the χ of $BaCu_2Si_2O_7$ shows a slight upturn and then drops suddenly around 10 K, while for $BaCu_2Ge_2O_7$ a similar upturn is followed by a steep increase below 10 K and finally by a saturation as shown in the inset to Fig. 3.

TABLE 2
Fractional Atomic Coordinates and Atomic Displacement Parameters for $BaCu_2Ge_2O_7$

Atom	Wyckoff position	x	y	z	B_{iso}(Å^2)
Ba	4c	− 0.0210(2)	0.25	0.9485(1)	0.59(3)
Cu	8d	0.2172(3)	0.0040(2)	0.7980(3)	0.63(4)
Ge	8d	− 0.0077(3)	0.1305(1)	0.4710(3)	0.19(3)
O1	4c	0.1007(11)	0.25	0.4831(13)	0.08(27)
O2	8d	− 0.1884(9)	0.1364(6)	0.6341(9)	0.99(21)
O3	8d	− 0.0563(10)	0.1143(6)	0.2357(8)	0.94(22)
O4	8d	0.1696(8)	0.0476(5)	0.5365(12)	0.49(20)

Note. Space group *Pnma*; $a = 7.04765(6)$ Å, $b = 13.40700(9)$ Å, $c = 7.02755(5)$ Å; $Z = 4$.

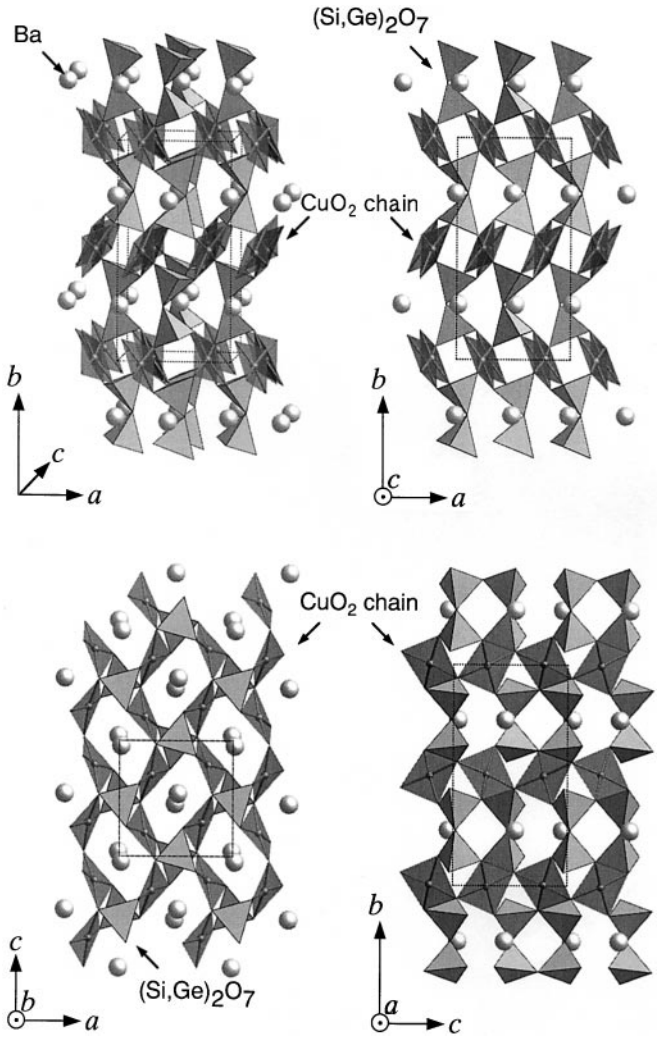

FIG. 2. Schematic representation of the crystal structure for $BaCu_2(Si_{1-x}Ge_x)_2O_7$. Corner-sharing, corrugated CuO_2 chains exist along the c axis with $(Si,Ge)_2O_7$ groups and Ba ions intervening. Significant interchain magnetic interactions are expected along the a axis.

The broad maximum at high temperature could be reproduced by assuming that

$$\chi = \chi_0 + \chi_{CW} + \chi_{1DHAF},$$

where χ_0 is the temperature-independent term coming from the core diamagnetism and the Van Vleck paramagnetism, χ_{CW} is the Curie–Weiss contribution ($\chi_{CW} = C/(T - \Theta)$), the origin of which will be discussed later, and χ_{1DHAF} is the spin susceptibility for the 1D HAF chains. For χ_{1DHAF} the following parametrized function which can reproduce the numerically calculated results by Bonner and Fisher (9) was used,

$$\chi_{1DHAF} = ((Ng^2\mu_B^2)/k_BT)(A + By^{-1} + Cy^{-2})$$

$$/(1 + Dy^{-1} + Ey^{-2} + Fy^{-3}),$$

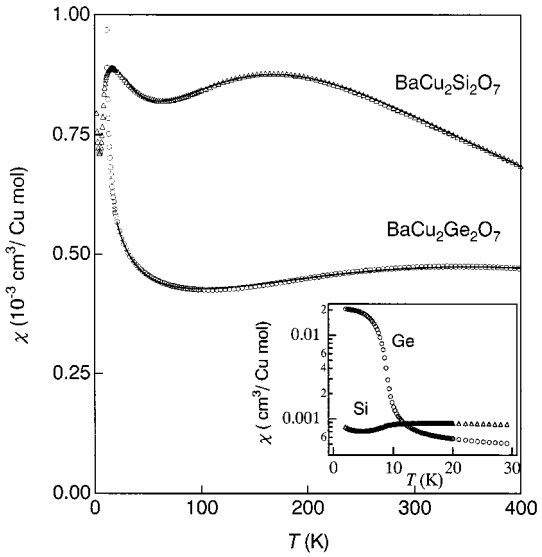

FIG. 3. Temperature dependence of magnetic susceptibility χ for $BaCu_2Si_2O_7$ and $BaCu_2Ge_2O_7$, which was measured with increasing temperature from 2 to 400 K in a magnetic field of 1 kOe. The solid line on each data set is a fit to the model described in the text. The inset shows a semilogarithmic plot of the same data at low temperature.

where $A = 0.250654$, $B = 0.0398637$, $C = 0.025211$, $D = 0.361143$, $E = 0.224491$, and $F = 0.142647$, $y = k_B T/J$, g is the g-factor, μ_B is the Bohr magneton, and k_B is the Boltzmann constant. The g-factor was fixed at 2.1 in each case which is a typical value for cupric oxides. Fitting was done at $T > 30$ (20) K for the Si (Ge) compound.

The obtained parameters are listed in Table 3. The AF coupling J was determined to be 291 (578) K for the Si (Ge) compound, 2 times larger for $BaCu_2Ge_2O_7$. The value for $BaCu_2Si_2O_7$ is in good agreement with that estimated from neutron scattering experiments ($J = 24.1$ meV $= 280$ K). This tendency is actually consistent with the above discussion on the relation between J and the Cu–O–Cu bond angle ($\theta = 121^\circ$ (Si) and 128° (Ge)). Moreover, it would be remarkable if such a small change in θ gives rise to the observed large difference in J. It is noted, however, that J is also very sensitive to θ around 90° in such a way that $J = -100$ K ($\theta \approx 94^\circ$) and 140 K for $CuGeO_3$ ($\theta = 99^\circ$). An additional factor to be possibly taken into account is another superexchange pathway through $Si(Ge)O_4$ tetrahedra to which the $2p$ (Si) or the $3p$ orbitals (Ge) would contribute. It is proposed that in a similar superexchange pathway seen in $CuGeO_3$ the $3p$ orbitals of Ge^{4+} are mixed with oxygen $2p$ orbitals and thus play an important role in the superexchange interactions between Cu^{2+} spins. This may be the case for the present Ge compound also, while the shallow $2p$ orbitals of Si^{4+} would not contribute so much in the Si compound.

TABLE 3

Antiferromagnetic Interaction J, Curie Constant C, Weiss Temperature Θ, and Temperature-Independent Susceptibility χ_0 Obtained from Fitting the Susceptibility Data for $BaCu_2(Si_{1-x}Ge_x)_2O_7$

x	J/k_B (K)	C (cm³ K/mol Cu)	Θ (K)	χ_0 (cm³/mol Cu)
0	291.3	0.0126	− 18.2	-2.16×10^{-5}
0.025	306.2	0.0202	− 21.4	-4.95×10^{-5}
0.05	309.3	0.0231	− 21.1	-5.43×10^{-5}
0.075	319.0	0.0213	− 17.9	-2.56×10^{-5}
0.1	320.3	0.0166	− 12.2	-3.56×10^{-5}
0.15	334.1	0.0210	− 14.2	-5.14×10^{-5}
0.25	370.1	0.0328	− 17.17	-7.89×10^{-5}
0.5	437.3	0.0246	− 11.7	-4.17×10^{-5}
0.75	498.0	0.0140	− 6.79	-2.99×10^{-5}
0.9	537.1	0.00726	− 2.57	4.77×10^{-6}
0.95	558.9	0.00718	− 2.88	1.65×10^{-5}
1	578.4	0.00483	− 0.97	4.34×10^{-5}

The anomalies observed at low temperature are probably due to the development of a magnetic LRO. In general, quasi-1D compounds exhibit LRO at low temperature owing to small interchain interactions. In the case of Sr_2CuO_3 the LRO occurs at $T_N = 5.4$ K so that $k_B T_N/J \approx 2.5\times10^{-3}$. The field dependence of magnetization M is nearly linear for $BaCu_2Si_2O_7$, while $BaCu_2Ge_2O_7$ shows a nonlinear hysteretic behavior (Figs. 4a, 4b) revealing the ferromagnetic nature of this oxide. The weak ferromagnetic moment is estimated to be 6.5×10^{-3} μ_B/Cu. Since the inversion center between adjacent Cu^{2+} ions is missing, the Dzyaloshinsky–Moriya interaction (10) is expected to lead to spin canting. That is, the weak ferromagnetism of $BaCu_2Ge_2O_7$ can be due to canted antiferromagnetism. In contrast, $BaCu_2Si_2O_7$ seems to exhibit an ordinary AF order without net moment. This striking difference between the two isostructural crystals should be explained reasonably. We will come back to this point later.

Specific heat. In order to get more insight into the magnetic phase transitions, we have measured the specific heat C which is usually a more sensitive indicator of phase transition than magnetic susceptibility. The results are shown in Fig. 5, where C/T is plotted against T, together with the corresponding changes of the derivative of χ–T curves. A small but distinct peak of C is seen around 9 K for each compound, which exactly corresponds to the inflection point seen in the χ–T curve. Consequently the peak in C indicates the occurrence of magnetic order, and the critical temperature T_N was determined from the peak-top temperature to be 8.9 K and 8.6 K for the Si and Ge compounds, respectively.

The peak in the specific heat for each compound is considerably small and broad, suggesting that the transition is

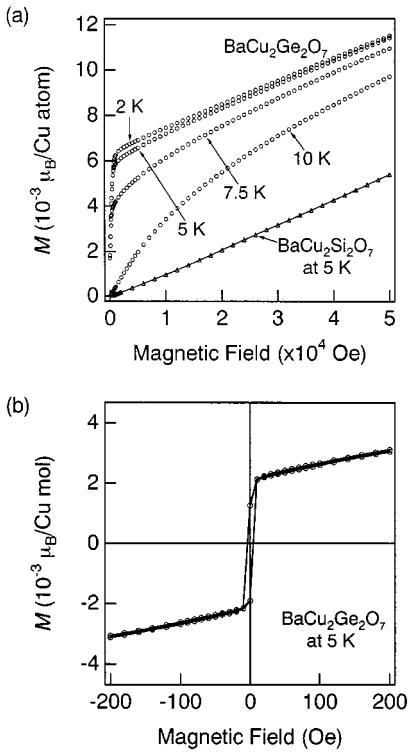

FIG. 4. Magnetization M versus magnetic field H for $BaCu_2Si_2O_7$ and $BaCu_2Ge_2O_7$ up to 50 kOe (a) and a hysteresis loop at 5 K for $BaCu_2Ge_2O_7$ (b).

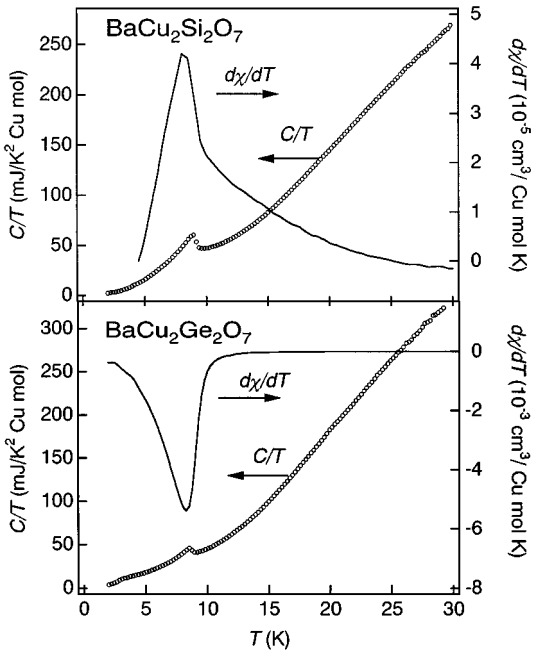

FIG. 5. Temperature dependence of specific heat C. C/T is plotted against T. Also shown is the corresponding derivative of $\chi(T)$.

of second order. This may exclude the possibility of any structural transition accompanying the magnetic transition. The small peaks as well as the low T_N's imply that most of magnetic entropy is lost by short-range ordering at high temperature below J/k_B, as generally seen in low-dimensional antiferromagnets. The smaller peak in the Ge compound should reflect its J being larger. Though quantitative discussion on the magnetic entropy was not possible because it was difficult to extract the lattice contribution precisely from the raw data, these specific heat data may be considered to support the picture that the present compounds are excellent quasi-1D systems with $k_B T_N/J = (1.5\text{–}3) \times 10^{-2}$.

As already mentioned, it is remarkable that the two isostructural compounds with nearly the same T_N's exhibit different types of magnetic order in a sense that a weak F moment is observed only for the Ge compound. Since the CuO chains are almost identical, it is likely that this difference arises from interchain coupling. We have carried out specific heat measurements in a static magnetic field up to 9 T, which might be similar to the interchain couplings in the energy scale. The results are summarized in Fig. 6. Surprisingly observed in $BaCu_2Ge_2O_7$ is that the peak at T_N is broadened with increasing magnetic field and, at the same time, another peak grows at 3–4 K. The 9 K peak is completely replaced by the one at 3.6 K at $H = 9$ T. Note that a shoulder was present around 3 K at $H = 0$ already. In striking contrast, the Si compound did not show such a dramatic field dependence, the 9 K peak being shifted to lower temperature by about 0.2 K only. It is interesting to note that the initial weakly F ground state of $BaCu_2Ge_2O_7$ is replaced by another one at high magnetic field, while the simple AF order in $BaCu_2Si_2O_7$ is robust. This fact must be related substantially to the nature of interchain couplings.

Solid Solutions $BaCu_2(Si_{1-x}Ge_x)_2O_7$

Crystal chemistry. We prepared solid solutions $BaCu_2(Si_{1-x}Ge_x)_2O_7$ with $x = 0.025$–0.95 and found that there is no miscibility gap between the parent compounds. The lattice parameters determined by the Rietveld refinements change linearly with x as expected from Vagard's law (Fig. 7). The ionic radius of a tetrahedrally coordinated Si^{4+} ion is 0.26 Å, and that of a Ge^{4+} ion is 0.39 Å. The observed lattice expansion with increasing x can be ascribed to this ionic size difference. To be noted here is that the c axis, which is the chain axis, expands with x as the other axes do. This seems to be against the general tendency for a substituted 1D chain compound to expand or contract little along the chain direction, if the valence of copper ions is not altered by the substitution. In the present compounds, however, the expansion of the c axis may result from the change in the bond angle θ, not from the change in Cu–O bond

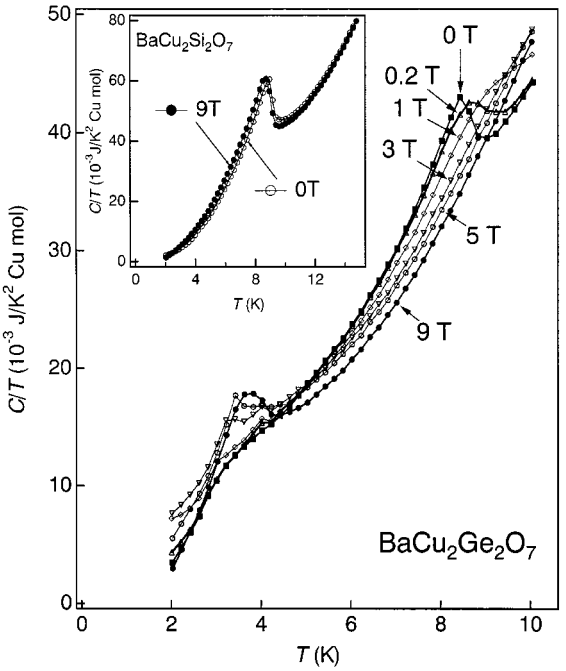

FIG. 6. Specific heat measured under magnetic field up to 9 T for $BaCu_2Ge_2O_7$ and $BaCu_2Si_2O_7$ (inset).

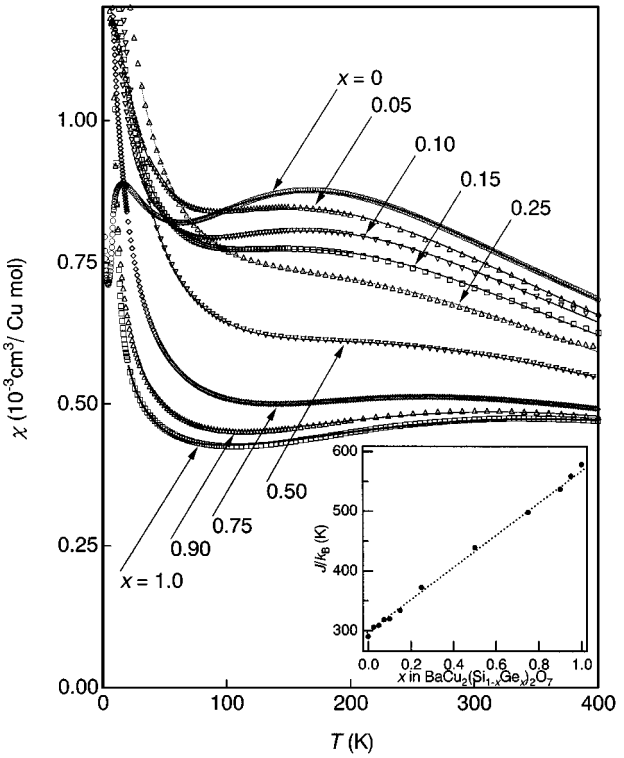

FIG. 8. Magnetic susceptibility for $BaCu_2(Si_{1-x}Ge_x)_2O_7$. A solid line on each set of data points is a fit to the model described in the text. The inset presents the composition dependence of the interchain interaction J showing a linear variation with x.

length, and it is the controllability of θ that leads to the change in J.

Magnetic properties. The magnetic susceptibility of the solid solution changes systematically with composition as shown in Fig. 8: the position of the broad maximum gradually shifts to higher temperature and the height becomes lower with increasing x. Fitting of χ was done as for the two end members to evaluate J. The results are summarized in Table 3 and the inset to Fig. 8. The J parameter has been found to increase almost linearly with x.

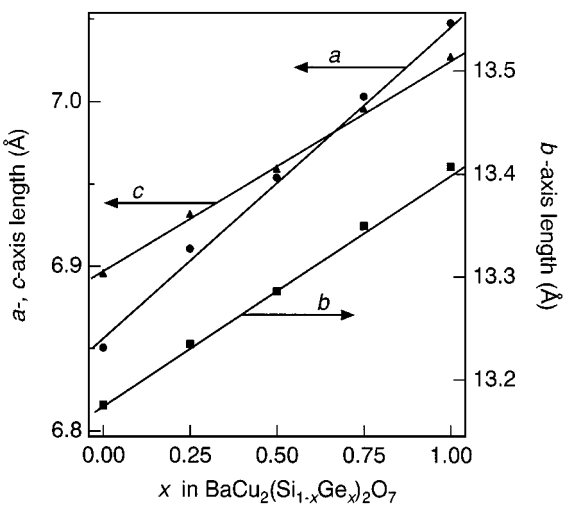

FIG. 7. Composition dependence of the lattice parameters for $BaCu_2(Si_{1-x}Ge_x)_2O_7$.

Next, we have investigated how the substitution affects the low-temperature magnetic order and how the two different types of order for the end members are interconnected. Figure 9 shows the composition dependence of the χ–T curve for $0 \leq x \leq 0.25$ (a) and $0.25 \leq x \leq 1$ (b). On the Si side the kink at 8.9 K (T_{N1}) tends to fade away with increasing x, and instead another peak grows at lower temperature (T_{N2}), the position shifting to lower temperature as x increases. These two anomalies coexist in the samples of $x = 0.025$ and 0.05. The Curie-like divergence which is already present in the Si compound apparently increases with x. On the Ge side the ferromagnetic increase in χ shifts to lower temperature and disappears for $x < 0.9$. On the other hand, there are neither AF nor F anomalies for intermediate compositions of $0.25 \leq x \leq 0.75$ above 2 K.

Specific heat. The composition dependence of specific heat is shown in Fig. 10, where substantially the same features can be seen as for χ. Two peaks at 9 K and 5 K coexist for $x = 0.025$, and a trace of the 9 K peak is discernible up to $x = 0.15$. The low-temperature peak shifts to

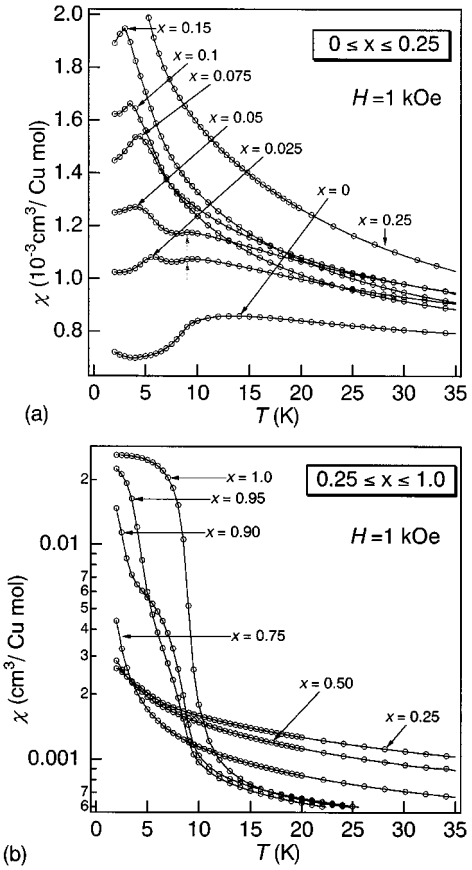

FIG. 9. Magnetic susceptibility at low temperature for $BaCu_2(Si_{1-x}Ge_x)_2O_7$ with $0 \le x \le 0.25$ (a) and $0.25 \le x \le 1$ (b).

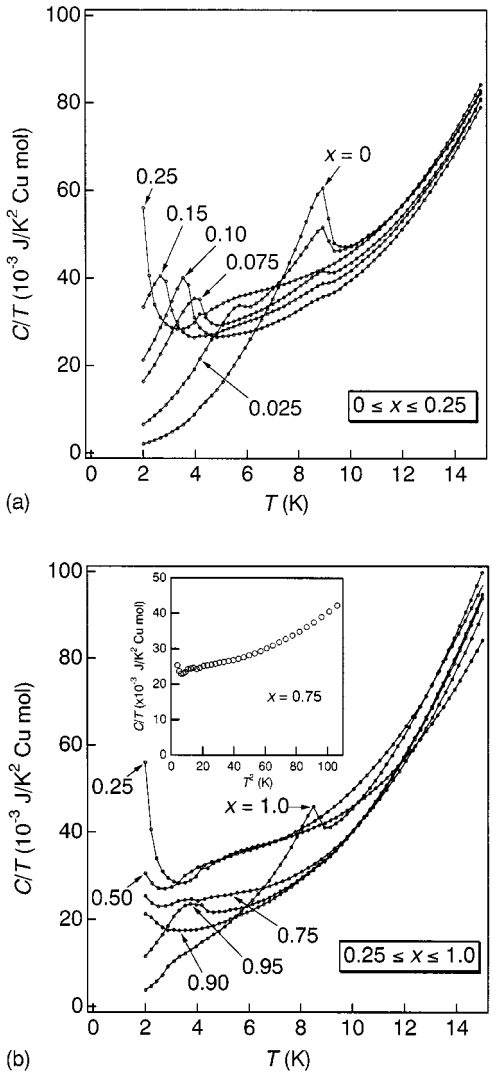

FIG. 10. Specific heat divided by T versus T plot for $BaCu_2(Si_{1-x}Ge_x)_2O_7$ with $0 \le x \le 0.25$ (a) and $0.25 \le x \le 1$ (b). The inset shows specific heat divided by T versus T^2 plot for the sample of $x = 0.75$, implying that a large T-linear contribution remained at low temperature.

lower temperature as x increases, down to below 2 K for $x = 0.25$ for which a steep leading increase is visible near 2 K. On the Ge-rich side, the composition dependences of the transitions are seen to be more clearly comparable with the magnetic data where the presence of spontaneous magnetization tends to prevent the transitions being detected clearly. The peak at 8.5 K for $x = 1$ disappears completely for $x = 0.95$ and instead another peak is seen at 4 K as on the Si-rich side. However, the low-temperature peak seems to appear only below 2 K even at $x = 0.90$.

It is interesting to notice that a nearly flat temperature dependence is seen below 5 K for $x = 0.75$, suggesting that the specific heat contains a large T-linear term. The inset of Fig. 10b shows a C/T versus T^2 plot for $x = 0.75$, which shows an almost linear behavior as T approaches zero, although a sudden jump follows below 2.4 K. Specific heat for 1D HAF chains is generally approximated to take the form $C = \gamma T$ at low temperature ($T \ll J/k_B$) (11). The actual C is the sum of the magnetic and lattice contributions; $C = \gamma T + \beta T^3$. Thus, the intercept of C/T versus T^2 gives a γ value which is assumed to be $2Nk_B^2/(3J)$. The inset graph gives $\gamma \approx 23\,\mathrm{mJ/K^2\,mol}$ Cu which corresponds to $J/k_B \approx 240$ K. This value is about a half of $J/k_B = 498$ K estimated from the $\chi(T)$ data. The discrepancy must come from the overestimation of γ for the following reason. Since there is apparently the Curie–Weiss contribution in the χ–T data, a considerable amount of Schottky-type specific heat must be involved in the $C(T)$ data. To be stressed here, however, is that this special sample may give an almost ideal $S = 1/2$ HAF chain system without any magnetic order above 2 K ($k_B T_N/J \le 4 \times 10^{-3}$). It is quite likely that interchain interactions are effectively diminished around $x = 0.75$. It might be possible to realize perfect, isolated 1D chains in a sample with a certain composition near $x = 0.75$ where AF and F interchain interactions cancel each other

and, therefore, quantum critical phenomena could be studied experimentally.

DISCUSSION

Magnetic Phase Diagram

We have clarified that $BaCu_2Si_2O_7$, $BaCu_2Ge_2O_7$, and their solid solutions $BaCu_2(Si_{1-x}Ge_x)_2O_7$ present a unique $S = 1/2$ 1D HAF system comprising corner-sharing but corrugated CuO chains with strongly composition (x)-dependent intrachain AF interactions. A tentative magnetic phase diagram at LT is illustrated in Fig. 11. A LRO sets in at $T_{N1}(\mathrm{Si}) = 8.9$ K for $x = 0$. As x increases, this transition tends to fade away and be replaced by another one with a lower $T_{N2}(\mathrm{Si})$ which decreases to below 2 K at $x = 0.25$. $BaCu_2Ge_2O_7$ exhibits an AF order with weak ferromagnetism at $T_{N1}(\mathrm{Ge}) = 8.6$ K. This transition is sensitive to applied field and the Si substitution as well, disappearing for $(x, H) = (1, 9\ \mathrm{T})$ and (0.95,0). Similarly to the case of the Si-rich side, a low-temperature transition appears at $T_{N2}(\mathrm{Ge}) \approx 4$ K and shows a peculiar field dependence.

Possible Model

The key to understanding the LT behavior is apparently the interchain interactions J'. The sensitivity of the transitions to magnetic field suggests that J' and H up to 9 T are of comparable magnitude. Coming back to the crystal structure illustrated in Fig. 2, significant interchain interactions are expected only along the a axis. The connection of adjacent chains is depicted also in Fig. 12, where neighboring chains shifts half-way from each other.

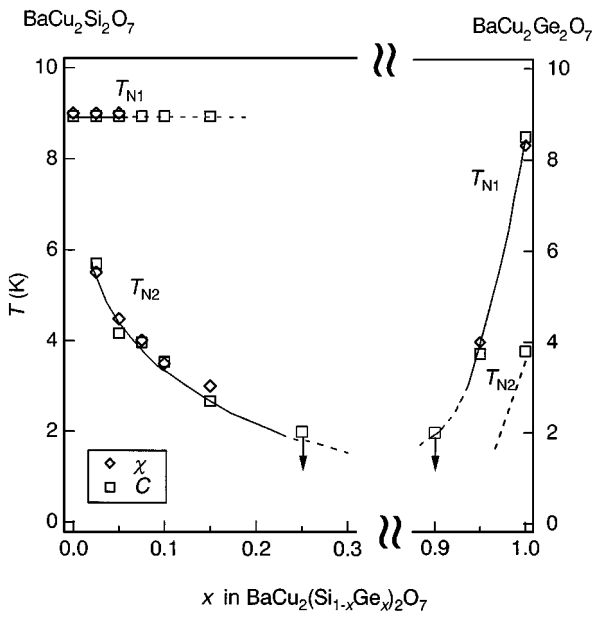

FIG. 11. Tentative magnetic phase diagram for $BaCu_2(Si_{1-x}Ge_x)_2O_7$. The transition temperatures marked with diamonds and squares were determined from $\chi(T)$ and $C(T)$ data at low temperature.

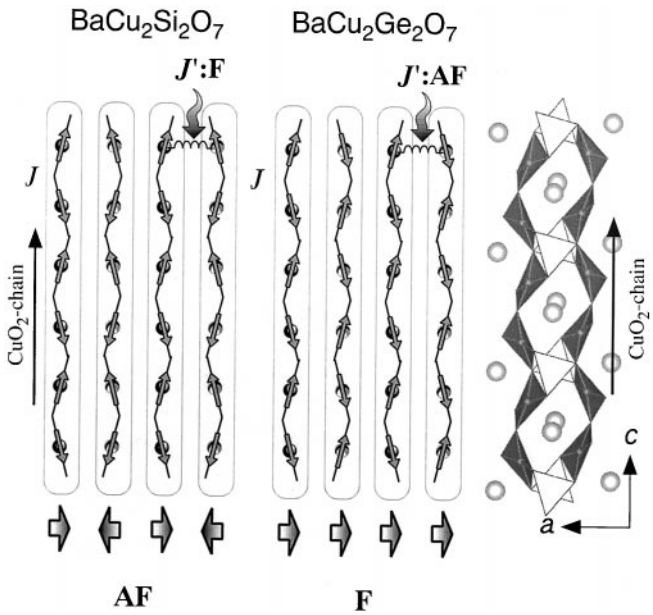

FIG. 12. Possible model for the spin arrangement realized in $BaCu_2(Si_{1-x}Ge_x)_2O_7$. The small arrows indicate $S = 1/2$ spins on Cu ions and the large ones are the weak net moments arising from the Dzyaloshinsky–Moriya interaction. The interchain interactions are ferromagnetic for the Si compound, while they are antiferromagnetic for the Ge compound. A weak ferromagnetic moment appears only for the Ge compound.

Our model is made of the following two factors. First, every chain has a weak net moment caused by the Dzyaloshinsky–Moriya interaction. Second, the interchain interaction is AF for the Ge compound but F for the Si compound. Illustrated in Fig. 12 is a possible spin structure where each spin is assumed to be in the CuO_4 plane and nearly parallel to the c axis as suggested by Tsukada *et al.*'s study on a single crystal with $x = 1$ (5). The net chain moment, M_{chain}, is canceled in the Si compound but is summed up in the Ge compound. The LRO due to interchain interaction will be strongly influenced by external field if the magnitude of $-M_{\mathrm{chain}}H$ becomes comparable with J', leading to the broadening and/or the disappearance of the magnetic and thermal anomalies due to the LRO. In this respect single crystals are highly needed because the present experiments using powdered samples leave ambiguity for the random orientation of the field relative to the spin axis.

In the solid solutions the interchain interactions of opposite signs may be mixed locally. It is easy to suppose that the interaction is, on average, reduced and, therefore, the magnetic ordering temperature is lowered. However, the appearance of the well-defined second transition at T_{N2} strongly suggests the occurence of another type of LRO with a

modified spin structure, probably of a long period along the a axis like up–up–down. The field dependence of the second transition around $x = 1$, such that the external field enhances the second transition for the pure Ge compound but suppresses it for $0.05 \leq x \leq 0.95$, also may be taken as suggesting a strong composition dependence of the spin structure. Here we note the possibility that J' is completely canceled at certain intermediate compositions like $x = 0.75$ so that no LRO occurs and the chains remain independent down to extremely low temperature. Concerning the Curie-like divergence below the broad maximum, it is considered that intrachain short-range ordering will induce a fluctuating net moment that looks like a free paramagnetic moment because the interchain interaction is weak.

CONCLUSIONS

We have shown that $BaCu_2(Si_{1-x}Ge_x)_2O_7$ represents a unique type of the $S = 1/2$ 1D HAF system with a tunable intrachain coupling between 290 K and 580 K depending on the Si/Ge composition. This feature originates in the corrugated and slightly retractable structure of the corner-sharing CuO_2 chains. In addition, a small interchain coupling also changes with the composition from ferromagnetic at the Si side to antiferromagnetic at the Ge side. It is pointed out, interestingly, that the interchain coupling can be diminished near $x = 0.75$, where almost completely magnetically isolated chains would be expected.

ACKNOWLEDGMENTS

This work was supported by CREST (Core Research for Evolutional Science and Technology) of the Japan Science and Technology Corporation and by a Grant-in-Aid for Scientific Research (C) of the Ministry of Education, Science, Sports and Culture.

REFERENCES

1. M. Hase, I. Terasaki, and K. Uchinokura, *Phys. Rev. Lett.* **70,** 3651 (1993).
2. C. Kim, Z.-X. Shen, N. Motoyama, H. Eisaki, S. Uchida, T. Tohyama, and S. Maekawa, *Phys. Rev. B* **56,** 15589 (1997).
3. Y. Mizuno, T. Tohyama, S. Maekawa, T. Osafune, N. Motoyama, H. Eisaki, and S. Uchida, *Phys. Rev. B* **57,** 5326 (1998).
4. J. Jaczak and R. Kuciak, *Acta Crystallogr. C* **46,** 1383 (1990).
5. I. Tsukada, Y. Sasago, K. Uchinokura, A. Zheludev, S. Maslow, G. Shirane, K. Kakurai, and E. Rssouche, *Phys. Rev. B* **60,** 6601 (1999).
6. T. Yamada, M. Takano, and Z. Hiroi, in *the proceedings of SCTE2000*, *Stresa*, *Italy*, *2000*.
7. F. Izumi, *in* "The Rietveld Method" (R. A. Young, Ed.), p. 236. Oxford Univ. Press, Oxford, 1993.
8. N. Motoyama, H. Eisaki, and S. Uchida, *Phys. Rev. Lett.* **76,** 3212 (1996).
9. J. C. Bonner and M. E. Fisher, *Phys. Rev.* **135,** A640 (1964).
10. I. Dzyaloshinsky, *J. Phys. Chem. Solids* **4,** 211 (1958).
11. K. Takeda, S. Matsukawa, and T. Haseda, *J. Phys. Soc. Jpn.* **30,** 1330 (1971).